Journal of Solid State Chemistry **158,** 82–86 (2001)
doi:10.1006/jssc.2001.9091, available online at http://www.idealibrary.com on IDEAL®

High-Pressure Synthesis and Electrochemical Investigation of $Ag_2Cu_2O_3$

K. Adelsberger, J. Curda, S. Vensky, and M. Jansen[1]

Max-Planck-Institut für Festkörperforschung, Heisenbergstrasse 1, D-70569 Stuttgart, Germany

Received August 2, 2000; in revised form January 2, 2001; accepted January 19, 2001

Single crystals of $Ag_2Cu_2O_3$ were prepared by solid state reaction of Ag_2O and CuO applying an oxygen pressure of 200 MPa. Crystals of $Ag_2Cu_2O_3$ ($I4_1/amd$, $a = 589.78(6)$, $c = 1071.4(2)$ pm from single crystal data, $Z = 4$, 289 unique diffractometer data, $R1 = 0.043$, $wR2 = 0.098$) are black and stable in air and moisture. The refinement of the crystal structure confirms previous results as obtained from powder data; however, the process has lead to improved precision. Electrochemical deintercalation experiments have been performed. From electrotitration curves and structural investigations on the resulting deintercalated phases we have been able to deduce an irreversible "single phase mode" deintercalation mechanism.

Key Words: **single crystal; silver cuprate; deintercalation; electrochemistry.**

INTRODUCTION

Principally, there are two approaches for overcoming the difficulties arising in the synthesis of multinary oxides of noble metals due to their inherent thermal labilities. One can either design a reaction that proceeds at low temperatures (below the decomposition temperature) at ambient pressure, or one can apply oxygen pressures high enough to overcompensate the oxygen equilibrium pressure during reaction in the solid state. Both routes have been widely used in the past. Examples for the former included electrocrystallization of binaries (Ag_2O_3, Ag_3O_4 (1, 2)) as well as precipitation (Ag_2PbO_2 (3, 4)) from an aqueous solution, while, e.g., $Ag_4Bi_2O_5$ (5) or $AgBO_2$ (6) are only accessible via the latter. Indeed, it seems as if for a given compound, only one of the two routes applies. Here we report on a high-temperature synthesis of single-crystalline $Ag_2Cu_2O_3$, which was previously obtained by a low-temperature reaction as microcrystalline powder (7). As this phase seems to meet topological and transport requirements for electrochemical deintercalation we have performed respective investigations. Numerous reports on electrochemical deintercalation have been published in the past due to interest in some of these compounds as positive electrode for high-energy density batteries (8, 9). Moreover, it has been shown that electrochemical oxidation can be a tool for tuning T_C in superconductors (10).

[1]To whom correspondence should be addressed. E-mail: martin@jansen.mpi-stuttgart.mpg.de.

EXPERIMENTAL

Synthesis

Black crystals of $Ag_2Cu_2O_3$ were prepared by solid state reaction of Ag_2O (precipitated from an acidic $AgNO_3$ solution) and CuO (Aldrich, 99%) in a high oxygen pressure. The binary oxides were mixed in a 1:1 molar ratio and then annealed for 3–5 days in silver crucibles placed in stainless steel autoclaves. The optimized reaction temperature and oxygen pressure are 500°C and 200 MPa, respectively. One milliliter of a 7 M KOH aqueous solution was added as an accelerator.

Microcrystalline, black powder of $Ag_2Cu_2O_3$ was precipitated from an aqueous solution of $AgNO_3$ (Merck, p.a., 99.5%) and $CuNO_3 \cdot 3H_2O$ (Panreac. p.a., 99.98%) adding 4 ml NaOH solution (3M). The precipitate was dried in air at 90°C for 24 h (7). The product was characterized by X-ray powder diffraction.

Structure Determination

Data collection on a single crystal of $Ag_2Cu_2O_3$ was performed on a Stoe Stadi4 four-circle diffractometer supplied with a graphit monochromator using Mo$K\alpha$ radiation ($\lambda = 71.069$ pm). Essential crystal data and experimental details of the structure determination are listed in Table 1. The structure was solved by the Patterson technique (SHELXS 86 (11)) and refined by full-matrix least-squares methods (SHELXL 97 (12)). The results of the X-ray crystal structure determination, such as atomic parameters and thermal parameters are documented in Table 2.

0022-4596/01 $35.00

TABLE 1
Crystal Data and Structure Determination of $Ag_2Cu_2O_3$

Crystal	black crystal of 0.1*0.1*0.1 [mm^3]
Formula weight	390.84 g/mol
Space group	$I4_1/amd$ (No. 141)
Unit cell dimensions	$a = 589.78(6)$ pm
	$c = 1071.4(2)$ pm
Cell volume	$372.7(1) \times 10^6$ pm^3
Z	2
Calculated density	6.966 g/cm^3
Wavelength	Mo$K\alpha$
Theta range for data collection	4–37°
hkl (min/max)	$-7 < h < 7 - 10 < k < 10$
	$-18 < l < 18$
No. of reflections measured	954
No. of unique reflections	289
No. of parameters	16
Absorption coefficient	21.443 mm^{-1}
Corrections	Lorentz polarization, absorption
R_{int}^a	0.023
$R1$ ($I > 2\sigma$)^b	0.043
w$R2$ (all data)^c	0.098

$^aR_{int} = \sum| F_o^2 - F_o^2(\text{mean})|/\sum [F_o^2]$.
$^bR1 = \sum||F_o| - |F_c||/\sum|F_o|$.
$^cwR2 = (\sum[w(F_o^2 - F_c^2)^2]/\sum [w(F_o^2)^2])^{1/2}$.

The powder diffraction data of the deintercalated phases were collected using a STOE-Stadi P diffractometer (germanium monochromator, Cu$K\alpha$ radiation, $\lambda = 154.056$ pm, linear position sensitive detector, Si as an external standard). The structures of the deintercalated phases have been refined by profile analysis using the Rietveld method (program FULLPROF (13)). Essential data of the structure refinements of the deintercalated phases are listed in Table 3.

Electrochemical Deintercalation/Intercalation Experiments

The cyclic voltammetry experiments and determination of the cell voltage versus charge transferred were performed by means of a Mac-Pile system (14) using a two-electrode configuration in both the potentiodynamic and the galvanostatic mode. Electrochemical reactions were studied in a two-electrode swagelock laboratory cell (15). A silver metal foil was used as a negative plate. The pure educt phase $Ag_2Cu_2O_3$ was used as a positive electrode. Silver nitrate, dissolved in acetonitrile, was applied as a liquid electrolyte. The open circuit voltage versus elemental silver did not exceed 0.6 V, which is well below the limit of the electrolyte used. The electrotitration of charge carriers was carried out with a constant current density of 9 μA/cm^2. Periods of working potential alternate with periods of the open cell potential.

TABLE 2
Positional and Isotropic (U_{eq})^a/Anisotropic Displacement^b Parameters for $Ag_2Cu_2O_3$

atom	x	y	z	U_{eq}	U_{11}	U_{22}	U_{33}	U_{23}	U_{13}	U_{12}
Cu	0	0	0.5	12(1)	13(1)	13(1)	10(1)	8(1)	0	0
Ag	0	0	0	21(1)	19(1)	24(1)	19(1)	−1(1)	0	0
O(1)	0	0.25	0.375	9(2)	12(2)	12(2)	4(3)	0	0	0
O(2)	0	0.25	0.1369(7)	20(7)	16(3)	24(4)	19(4)	0	0	0

$^aU_{eq} = 1/3(U_{11} + U_{22} + U_{33})$.
^{b}The anisotropic displacement factor exponent takes the form: $-2\pi^2[U_{11}h^2a^{*2} + \cdots + 2U_{12}hka^*b^*]$.

TABLE 3
Change of Cell Parameters of Deintercalated $Ag_2Cu_2O_3$ as a Function of Charge

Charge [mA*h]	Cell volume [$Å^3$]	c [Å]	a [Å]
0	371.37(2)	10.6987(4)	5.8916(2)
1.90	371.13(2)	10.6979(8)	5.8900(3)
2.85	370.50(4)	10.6953(8)	5.8857(3)
3.33	370.44(4)	10.6932(7)	5.8858(3)
3.81	370.44(4)	10.6950(8)	5.8853(3)
4.28	370.22(4)	10.6926(7)	5.8842(3)
4.76	370.46(4)	10.6948(8)	5.8855(3)
5.23	370.11(4)	10.6930(8)	5.8833(3)
9.51	369.03(6)	10.6805(12)	5.8781(6)
11.42	369.60(7)	10.6838(13)	5.8817(6)
13.32	369.39(7)	10.6785(13)	5.8815(5)
15.22	366.18(9)	10.6514(17)	5.8633(8)

Magnetic Measurements

Magnetization of $Ag_2Cu_2O_3$ and of the deintercalated phases were recorded using a Squid magnetometer (Quantum Design MPMS; 5–300 K).

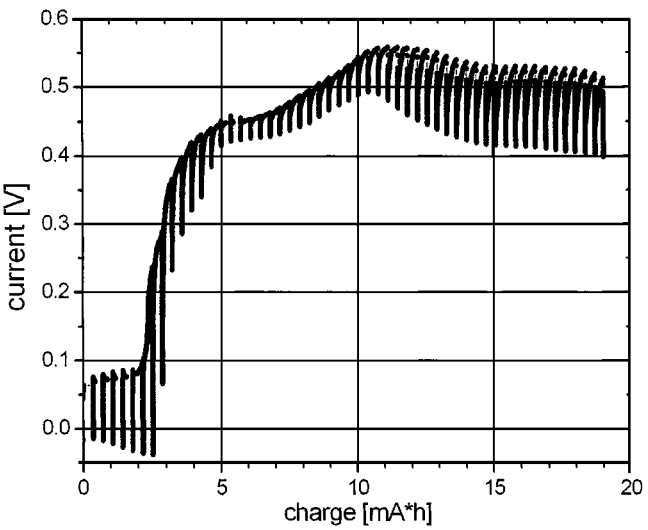

FIG. 1. Variation of the cell voltage versus charge for $Ag_2Cu_2O_3$.

TABLE 4
Ag/Cu Ratios of the Deintercalated Phases

Charge [mA*h]	Silver content calc. [w%]	Copper content calc. [w%]	Silver content exp. [w%]	Copper content exp. [w%]	Ag/Cu
0	55.2	32.5	52.7	33.4	1.9/2
4.76	48.6	38.1	46.0	39.3	1.4/2
5.71	46.3	39.0	43.4	41.0	1.3/2
7.61	42.5	41.7	41.6	42.4	1.16/2
11.42	33.0	48.6	41.9	41.8	1.18/2
13.32	27.0	53.0	42.3	41.5	1.2/2
15.22	19.8	58.3	41.1	43.6	1.1/2

Chemical Analyses

The cation ratio of the deintercalated samples of $Ag_2Cu_2O_3$ was determined by a ICP OES (Inductive Coupled Plasma Optical Emission Spectrometer/TJA, Offenbach, IRIS Advantage Spectrometer with Echelle-Optik and CID-detector, 177–1000 nm). Oxidation states of copper were determined iodometrically (18).

RESULTS AND DISCUSSION

Single crystals of $Ag_2Cu_2O_3$ have been obtained by reacting solid Ag_2O and CuO while applying an oxygen pressure of 200 MPa. Refinement of the crystal structure using single-crystal X-ray data of $Ag_2Cu_2O_3$ confirms previous results (7). However, since single-crystal data were used, the precision was improved significantly and anisotropic thermal parameters were determined. $Ag_2Cu_2O_3$ represents a heterometallic variant of the Cu_4O_3 type of structure (16) and consists of chains of edge-sharing, planar CuO_4 squares, which are interconnected via linear O–Ag–O units. The relatively low coordination numbers of the cationic constituents, the free space within the framework, and the notoriously high mobility of monovalent silver in solids makes $Ag_2Cu_2O_3$ a promising candidate for electrochemical deintercalation experiments. In particular, the opportunity offered by such investigations to create phases containing copper in a $+3/+2$ mixed valent state appeared attractive to us.

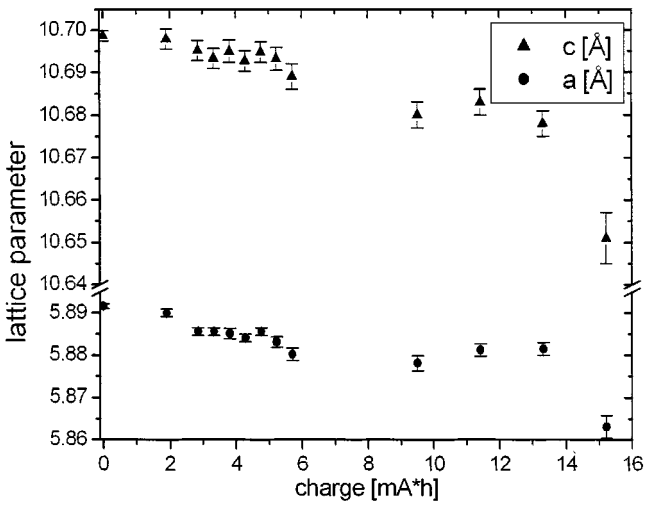

FIG. 2. Variation of the lattice parameters versus charge for $Ag_2Cu_2O_3$.

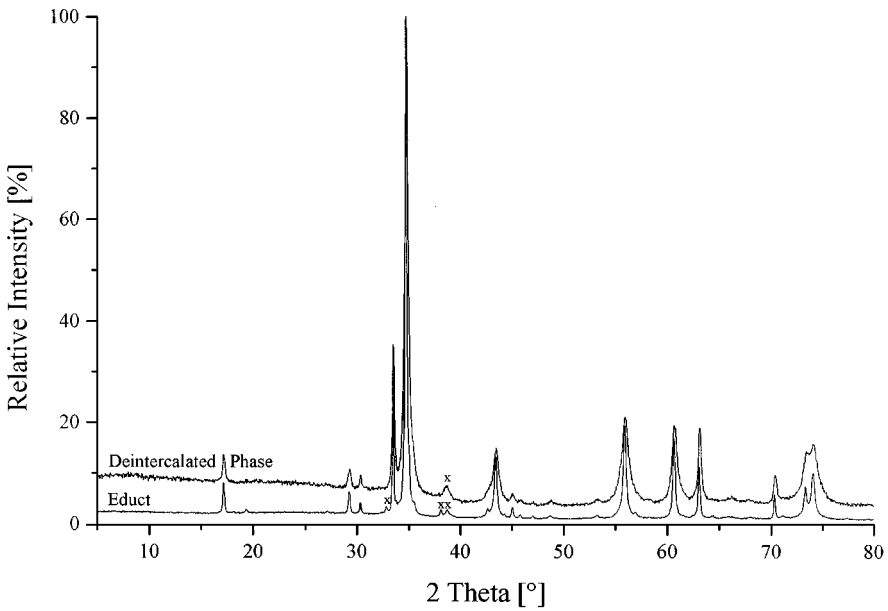

FIG. 3. Powder diffraction patterns of $Ag_2Cu_2O_3$: educt and deintercalated phase, asterisks mark reflections caused by Ag_2O and CuO.

The development of the cell voltage at a constant current of 0.01 mA at charging (Fig. 1) shows a continuous change of slope without any extended plateau. There are some features indicating significant changes in the deintercalation mechanisms while the cell is charged. So the electrotitration curve shows a small induction period ranging from 0 to 2.25 mA*h of charge transferred within which deintercalation of silver has been proven to be reversible. Starting with the steep increase of the cell potential at further charging, the process turns irreversible, and the deintercalation of silver is accompanied by a loss of oxygen. This interpretation is in accordance with the results of iodometric redox titration analysis and microthermogravimetry at the deintercalated phases, none of which gave any evidence for an increase of the Cu^{III} content.

The maximum of voltage occuring at 10.8 mA*h marks another change in the deintercalation mechanism. The Ag/Cu ratio as determined by chemical analysis confirms the steady loss of silver during charging the electrochemical cell up to this point (Table 4). At further charging the Ag/Cu ratio remains constant. Thus this maximum apparently indicates the upper limit to which the only charge carriers involved are the silver ions. Beyond this point, simultaneous migration of copper and silver cations occurs over the remaining range of charge transfer.

Rietveld evaluation of the powder diffraction data of deintercalated phases gives conclusive support to the discussed mechanisms of deintercalation, although the crystallinity of the powder samples worsens during the electrochemical reaction (Fig. 3). Over almost the whole deintercalation range powder patterns were obtained which show the characteristic intensity profile of $Ag_2Cu_2O_3$; however, the diffraction lines were shifted to higher angles at increasing amount of charge transferred. The cell parameters a and c as well as the volume decrease steadily with proceeding deintercalation (Fig. 2). Rietveld evaluation of the powder diffraction data of deintercalated phases was performed over the whole range of deintercalation. Figure 3 shows a comparison of the powder profiles of the starting material and a phase charged by 9.5 mA*h. The shifts of the diffraction lines toward higher Θ-values are clearly visible, as is the decrease in cristallinity.

$Ag_2Cu_2O_3$ is paramagnetic with an antiferromagnetic ordering temperature $T_N = 60$ K (Fig. 4a) (17). The magnetic properties of the deintercalated phases change continuously with the progress of deintercalation. The variation of the reciprocal molar susceptibility versus temperature of these phases illustrates that the characteristic antiferromagnetic–paramagnetic transition continuously diminishes and finally disappears when silver ions and, later on, copper ions are electrochemically removed (Figs. 4a–4c).

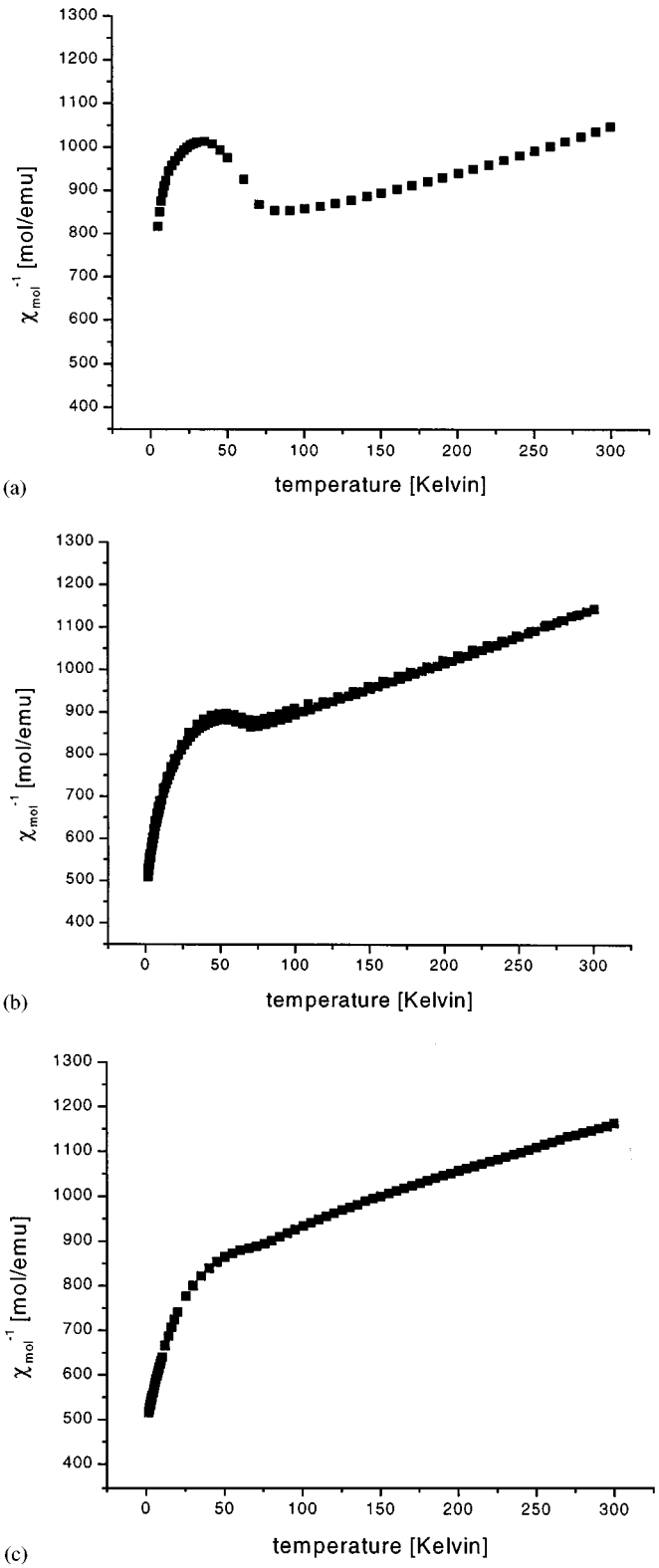

FIG. 4. Temperature dependence of the magnetic susceptibility of deintercalated phases referred to the charge (a) 0, (b) 9.51, and (c) 18.08 mA*h.

By EDX it has been proven that the samples are homogeneous at all stages of deintercalation and all grains contain copper and silver at the same time. It is worthwile mentioning that this is also true for the highest charged samples. Thus it has proven to be impossible to fully remove silver from $Ag_2Cu_2O_3$.

CONCLUSION

Single crystals of $Ag_2Cu_2O_3$ have been grown for the first time. Structure refinement based on single-crystal data has lead to improved precision of the structural data, and former results have been completed by the anisotropic thermal parameters. Electrochemical investigations on a pellet of $Ag_2Cu_2O_3$ arranged as a solid anode have revealed a complex deintercalation mechanism. Over the whole range of deintercalation the characteristic powder pattern of $Ag_2Cu_2O_3$ is maintained; however, the diffraction lines shifted to higher angles as the charge increased. The variation of the cell potential versus charge indicates a somewhat more complicated electrochemistry than deintercalation of a solid solution only. There is a short induction period of reversible deintercalation of silver up to 2.25 mA*h. At further charging, in addition to the deintercalation of silver, oxygen is evolved, while no Cu^{III} could be detected. Up to 10.8 mA*h the dominating charge carriers are silver ions. When the cell is charged beyond this value the current causes migration of copper, too, which has been proven by determining the Ag/Cu ratio of the deintercalated phases by chemical analyses. Rietveld refinements of the powder diffraction data of the deintercalated phases give support to these mechanistic interpretations.

ACKNOWLEDGMENT

Support by the Fonds der Chemischen Industrie is gratefully acknowledged.

REFERENCES

1. P. Fischer and M. Jansen, *Acta Chem. Scand.* **45,** 816 (1991).
2. P. Fischer and M. Jansen, *Inorg. Synth.* **30,** 50 (1995).
3. A. Byström and L. Evers, *Acta Chem. Scand.* **4,** 613 (1950).
4. M. Jansen, M. Bortz, and K. Heidebrecht, *Z. Kristallogr.* **186,** 147 (1989).
5. M. Jansen and S. Deibele, *Z. Anorg. Allg. Chem.* **622,** 539 (1996).
6. M. Jansen and G. Brachtel, *Naturwissenschaften* **67,** 606 (1980).
7. P. Gómez-Romero, E. M. Tejada-Rosales, and M. Rosa Palacín, *Angew. Chem.* **111,** 544 (1999); *Int. Ed.* **38,** 524 (1999).
8. C. Delmas, "NATO ASI SER, Ser. B," *Chem. Phys. Intercal.* **172,** 209 (1987).
9. Y. Chabre, "NATO ASI SER," *Chem. Phys. Intercal. II* **305,** 181 (1982).
10. S. Ondoño-Castillo, P. Gómez-Romero, A. Fuertes, and N. Casañ-Pastor, *Mater. Sci. Forum* **152–153,** 193 (1994).
11. G. Sheldrick, "SHELXS-86," University of Göttingen, Germany, 1986.
12. G. Sheldrick, "SHELXL-97," University of Göttingen, Germany, 1997.
13. J. Rodriguez-Carjaval, "FULLPROF 99," Version 0.3, Apr. 99. LLB-JRC, Laboratoire Leon Brillouin (CEA-CNRS), France, 1999.
14. C. Mouget and Y. Chabre, "McPile," licensed from CNRS and UJP Grenoble to BIO-LOGIC CO., av. de l'Europe, F-38640 Claix.
15. D. Guyomard and J. M. Tarascon, *J. Electrochem. Soc.* **139,** 937 (1992).
16. M. O'Keeffe and J. O. Bovin, *Am. Mineral.* **63,** 180 (1978).
17. P. Gómez-Romero, E. M. Tejada-Rosales, and M. Rosa Palacín, *in* "Proceedings of VIIth European Conference on Solid State Chemistry," Universidad Complutenses, Madrid, 1999.
18. G. Jander, K. F. Jahr, G. Schulze, and J. Simon, "Maßanalyse," Springer-Verlag, Berlin/New York, 1990.